http://journal.uir.ac.id/index.php/JGEET

E-ISSN : 2541-5794
P-ISSN : 2503-216X

Journal of Geoscience,
Engineering, Environment, and Technology
Vol 10 No 2 2025

RESEARCH ARTICLE

Seismic Hazard for Regional-Scale Sumatra Island Based on Realistic Physical Computation of Seismic Wave Propagation

Irwandi[1]*, Zulfakriza[2], Muzli[3], Hany M. Hassan[4,6], Makoto Okubo[5]

[1] Faculty of Math. and Natural Science, Universitas Syiah Kuala, Banda Aceh, Indonesia
[2] Global Geophysics Research Group, Faculty of Mining and Petroleum Engineering, Institut Teknologi Bandung
[3]Agency for Meteorology Climatology and Geophysics, Indonesia
[4]National Research Institute of Astronomy and Geophysics, NRIAG, 1 Marsad Street, Helwan, Cairo, Egypt
[5]Natural Science Cluster, Science and Technology Unit, Kochi University, 2-5-1, Akebono-cho Kochi, Japan
[6]National Institute of Oceanography and Applied Geophysics, OGS, Via Treviso 55, 33100, Udine, Italy

* Corresponding author : irwandi@usk.ac.id
Tel.:+62 85260104417
Received: March 18, 2025; Accepted: May 31, 2025.
DOI: 10.25299/jgeet.2025.10.02.21751

Abstract

Sumatra traversed by active fault zones leads to an earthquake's danger is a severe concern for the government as disaster mitigation efforts. The provision of a precise seismic hazard map attempts to recognize the hazard and the first step to start the disaster mitigation efforts. However, Indonesia's official hazard map has used the Probabilistic Seismic Hazard Analysis (PSHA) method based on general ground motion prediction equations (GMPE). General GMPE calculates strong ground motion, however, it has not been able to conduct a comprehensive study involving the focal mechanism's structural model and seismogenic zones. On the other hand, the Neo-Deterministic Seismic Hazard Assessment (NDSHA) method can integrate available geological, geophysical, seismological, and geotechnical information to calculate strong ground motion and applied in several countries successfully. Sumatra has oblique subduction causing a resultant force that triggers a right-lateral strike-slip fault activity called the GSF (Great Sumatran Fault). The high seismicity and focal mechanism complexity in Sumatra have been a challenge for implementing the method NDSHA. Structural models under the receiver site necessary for the realistic calculation of synthetic seismograms are divided into polygons aligned with the Sumatra coastline's general orientation. Regarding the data availability and resolution, the crust structural model gets from the LITHO1.0 model. The structural model compilation is validated as input for synthetic seismogram computation and verified by field observations of the instrument seismometer and accelerometer. Seismograms observation data from the Pidie Jaya earthquake on 7 December 2016 with a magnitude of M6.5 shows relatively good validity with synthetic seismograms. The success of synthetic seismogram validity makes us confident to apply strong ground motion calculations throughout Sumatra.

Keywords: Realistic Seismic Hazard Computation, Sumatra, NDSHA

1. Introduction

The collision of the Australian and Indian plates with the Euroasia plate will produce the Sunda subduction zone (SSZ) with the Sunda trench arc formation, which generates many significant earthquakes (Widiyantoro et al., 2024, Putra et al., 2023, Muksin et al., 2023) as shown in Fig. 1. No casualties were killed directly by the earthquake shaking, but killing them is a danger that resulted from the earthquake triggers such as tsunamis, landslides, and building collapse. The famous phrase "Earthquakes don't kill people, buildings do" (McKenna, 2011). Apart from the tsunami, many victims died because the buildings' quality was below the earthquake's estimated hazard. The author directly observed the Takengon earthquake M6.1 in 2012 and the Pidie Jaya earthquake M6.5 in 2016. Many buildings collapsed because their construction is not strong enough to face earthquakes ground shaking. Therefore, designing a building must consider the region's potential seismic hazard through the precise seismic hazard analysis (SHA) calculation and carefully reviewed. For instance, the official seismic hazard map when the Pidie Jaya happen, the probabilistic SHA (PSHA) underestimated the danger of the 2016 Pidie Jaya earthquake because ignoring the branching of GSF and has connected to the Mergui Basin, which was well known from several geological studies (Jacob et al., 2021, Bhat et al., 2023, Yadav and Tiwari, 2020).

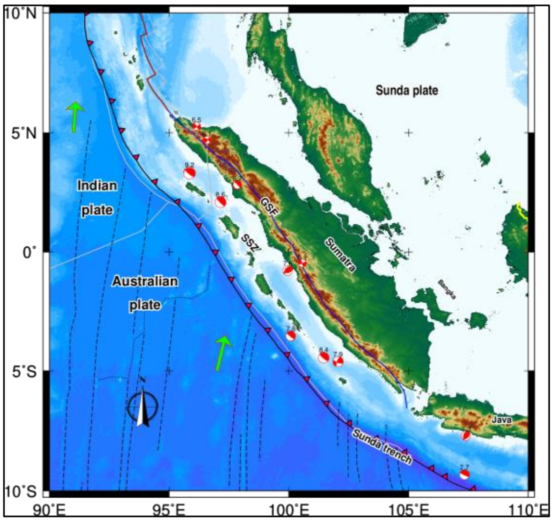

Fig.1. Sumatra tectonic setting and focal mechanism of the most deadly earthquakes in Sumatra.

Making an earthquake hazard map has challenges the difficulty not only identify active faults but also choosing the SHA method used to be crucial. For example, applying general gound-motion prediction equations (GMPE) (Irwandi et al., 2018a, Marzocchi and Meletti, 2024, Zanetti et al.,2023) for many area in probabilistic-based map making (PSHA) are considered unrealistic compared to calculating seismic field wave propagation depend on structural model (Irwandi et al., 2019). Some of the attenuation equations do not pay attention to the earthquake mechanism's information or focal mechanism.

Neo development Deterministic Seismic Hazard Assessment (NDSHA) have been conducted in Italy and other countries where seismic hazard is calculated has involved information geological, geophysical, and the mechanism of the earthquake (Panza and Bela, 2022, Elgabry et al., 2022, Zhang et al., 2021, Magrin et al., 2016, Hasan et al., 2017, Parvez et al., 2017, Pendiaman et al., 2024). Since the NDSHA method more realistic based on physical modeling than PSHA that rely on the general attenuation equation (Bahrampouri et al., 2021, Irsyam et al., 2020, Irwandi et al. 2021). This paper will discuss source definition, structural model, validation of synthetic seismogram, conducting regional-scale NDSHA for Sumatra.

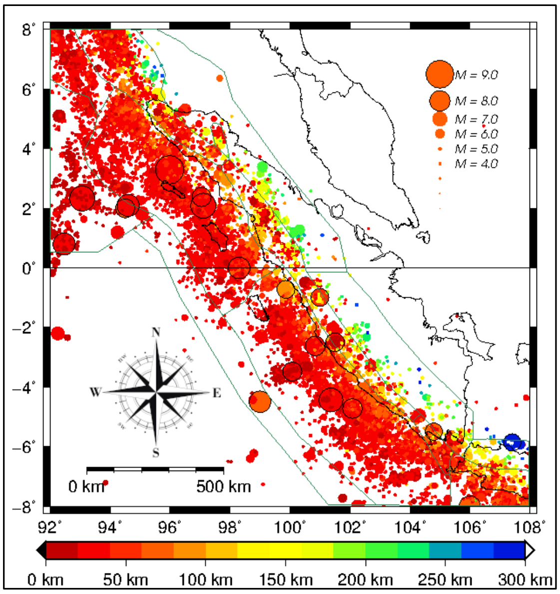

Fig 2. Seismicity for Sumatra is compiled from 1797-2022.

2. Methodology

This study employs the Neo-Deterministic Seismic Hazard Assessment (NDSHA) method developed by Panza et al. (2012). A comprehensive extraction of strong ground motion parameters is performed at receiver locations to generate a seismic hazard map.Unlike the Probabilistic Seismic Hazard Assessment (PSHA) method, which relies solely on the statistical attenuation equations of the Ground Motion Prediction Equation (GMPE), the NDSHA approach computes these parameters using realistic synthetic seismograms. This calculation integrates detailed information from the earthquake source and the structural model of the seismic medium. The outline of the NDSHA computation flow diagram is shown in Fig. 3.

The earthquake source information in this method includes magnitude, epicenter, and focal mechanism. A seismogenic zone map is developed based on tectonic setting data and the distribution of focal mechanism types (Fig. 4). For each seismogenic zone, the most representative focal mechanism is selected.The earthquake catalog used in this study is compiled from multiple sources, both global and regional, and then refined to focus on the research area. Additionally, an enhanced source smoothing process is applied to identify the most significant seismic sources within each grid of the seismogenic zones as shown in Fig. 5 (Irwandi, 2022).

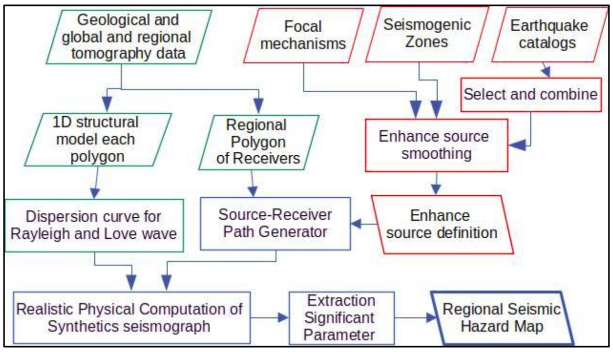

Fig. 3. The NDSHA procedure flowchart illustrates realistic seismic hazard analysis.

Realistic seismic wave propagation computation requires incorporating structural models at the receiver location. These models are constructed using available global and regional tomography data, where Vp (Fig. 6) and ρ are obtained from Pesicek, Vs from Sriwidiantoro, and attenuation (Qs) from global datasets (Dalton et al., 2008, Pesicek, et al., 2010, Pasyanos et al., 2014). Surface layer data, specifically the crustal structure, is derived by assimilating Litho 1.0 data. Each regional polygon (Fig. 7) is represented by a 1D structural model (Fig. 8a), which is then utilized to compute dispersion curves for Rayleigh (Fig. 8b) and Love waves (Fig. 8c).

From the information on the source and receiver points, source-receiver paths are generated and used as input for calculating synthetic seismograms (Fig. 9) and the respond spectral as shown in Fig. 10. This calculation is performed using the modal summation method as shown in equation 1, incorporating precomputed dispersion curves. At each receiver point, significant strong ground motion parameters are extracted, such as PGA (Peak Ground Acceleration), PGV (Peak Ground Velocity), and PGD (Peak Ground Displacement). Once calculations for all receiver points are completed, the results are compiled to generate a regional seismic hazard map, as shown in Fig. 11 for PGA.

2.1. Earthquake Source

Earthquake catalogs are relatively easy to obtain and publicly available information. The catalogs' available because of the basic requirement information for the public in time, focal location, and magnitude. This study combines several available catalogs from USGS, ISC, BMKG, and by Pesicek (Pesicek et al., 2010). United States Geological Survey (USGS) provides the most completed information but mostly in the preliminary determination of epicenters (PDE). Fig. 2 shows the plotting of the USGS data only without combining it with other catalogs. International Seismological Center (ISC) provides earthquake relocation information globally (Storchak et al., 2020).

After compiling the earthquake catalog containing information, time, location, and magnitude, additional required information for the point source computation is the focal mechanism in the format strike, dip, and rake. The easiest way to determine all earthquake focal mechanisms is to classify the earthquakes into a seismogenic zone. Design seismogenic polygon zones through comprehensive studies (Fadhlurrohman et al., 2024,Hutchings et al., 2021, Hu et al., 2023, Muksin et al., 2023, Rafie et al., 2023). With the QGIS software, we can investigate and identify more datail the clustering patterns of the strike, dip, and rake parameters as shown in beach ball focal mechanism in Fig. 4.

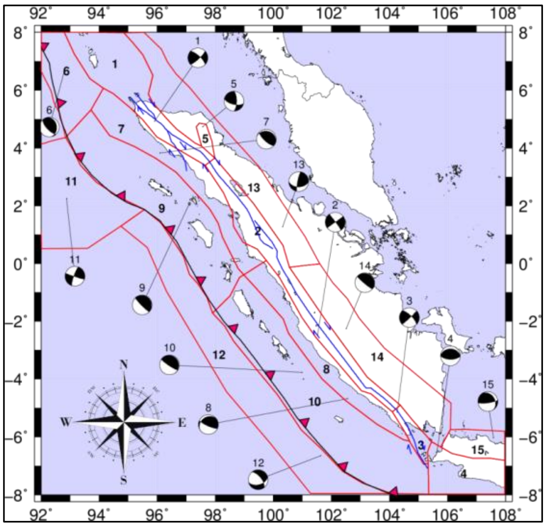

Fig. 4. Polygons of seismogenic zone with the associate focal mechanism.

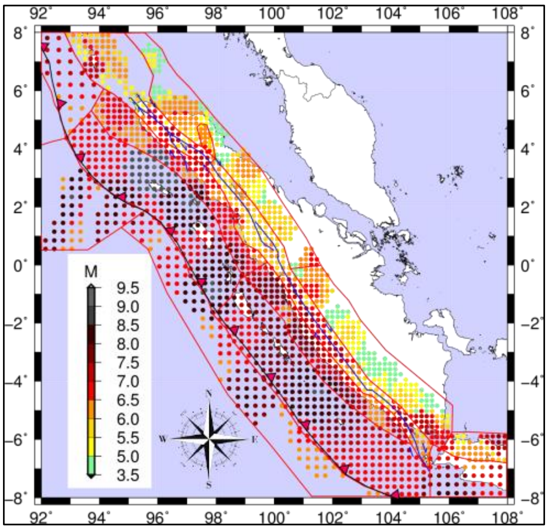

Fig. 5. Enhance source definition for Sumatra.

The NDSHA procedure calculates strong ground motion through by realistic simulation seismic wavefield propagation spend computational time. Therefore, for efficiency reason, the efficiency of the number of synthetic seismograms that must be computed should reduce to the optimum number of source by only calculating one MCE earthquake source for each source cell. On the other hand, measurement uncertainty and earthquake repetition do not occur at the same location, so we need to smoothing earthquake magnitude to closest neighboring cells with three categories of smoothing radius (Zhang et al., 2023). The paper explains that there are two essential parameters for carrying out earthquake smoothing, namely cell size and smoothing radius, that apply globally. Fig. 5 shows the application of the enchance smoothing of source procedure for Sumatra with a cell size of 0.2 degrees and a smoothing radius of 3 cell units that apply globally to all polygons.

2.2. Structural Model

One of the advantages of NDSHA over PSHA is the accuracy of strong ground motion calculations involving structural model information. The structural model will produce the dispersion curve needed in the modal summation technique to produce synthetic seismograms. The consequences would be paid by providing information for structural models for the subsurface information is needed to produce structural models at an observation point is ρ, Vp, Vs, Qp, and Qs, respectively the density, primary wave velocity, shear wave velocity, and wave attenuation for primary and shear wave. This data is in the form of a 1D structural model down to 1500km where receiver sites located in a polygon area. To provide the 1D structural model, global and regional tomography data is collected from many studies (Pesicek, et al., 2010, Pasyanos et al., 2014). The recent tomography studies for Sumatra Island (Liu et al., 2021, Osagie and Abir, 2021, Shamim et al., 2021, Wei et al., 2024). The Vp for surface layer as shown in Fig. 6 is plotted from tomography data.

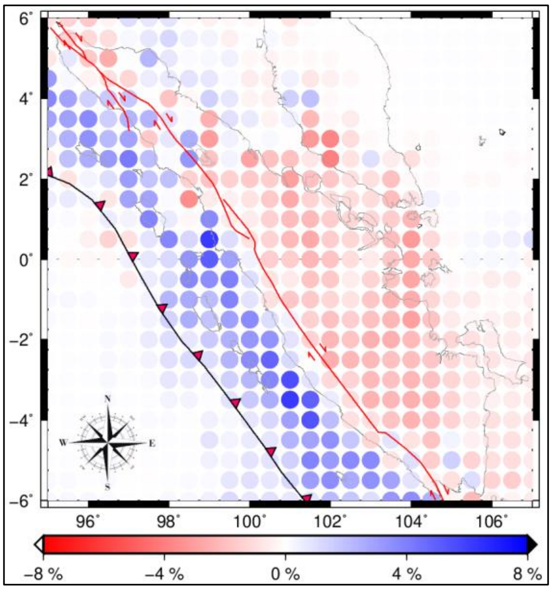

Fig. 6. Vp anomaly from regional tomography inversion (Pesicek et al. 2010)

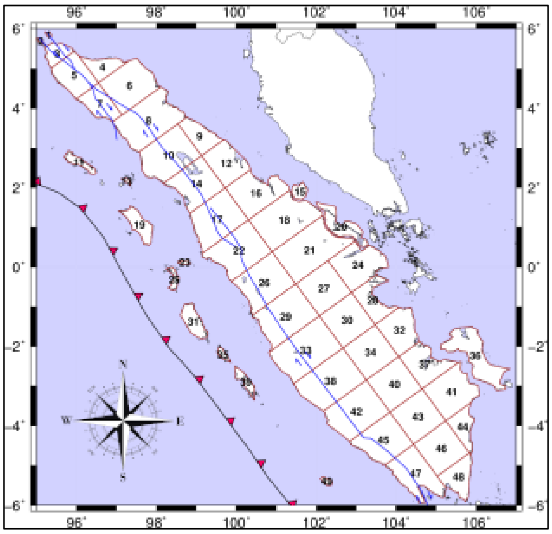

Fig. 7. Cellular polygons for classification and reducing number structural model for computation.

For the structural model we can calculate each point for a 0.5 degree grid as provided by tomography data. However, the number of structural models will be very large and we will calculate too many dispersion curves. Therefore, we reduce the number of structural models by dividing them into polygons that have similar structural models based on geological and structural model information (Natul et al., 2022, Dwikorianto et al., 2023, Amir et al., 2021, Adhari et al., 2023) and the polygon grouping results we obtain are shown in Fig. 7. From this polygon, we will take a point in the middle of the structural model to represent the structural model for that polygon. The results of the polygon compilation for the structural model are shown in Fig. 8a. The data compile from mass density, Vp, Vs, and attenuation. Based on the structural model, the dispersion curve for both Rayleigh waves and Love waves is calculated using non linear computation as shown in Fig.s 8b and 8c respectively.

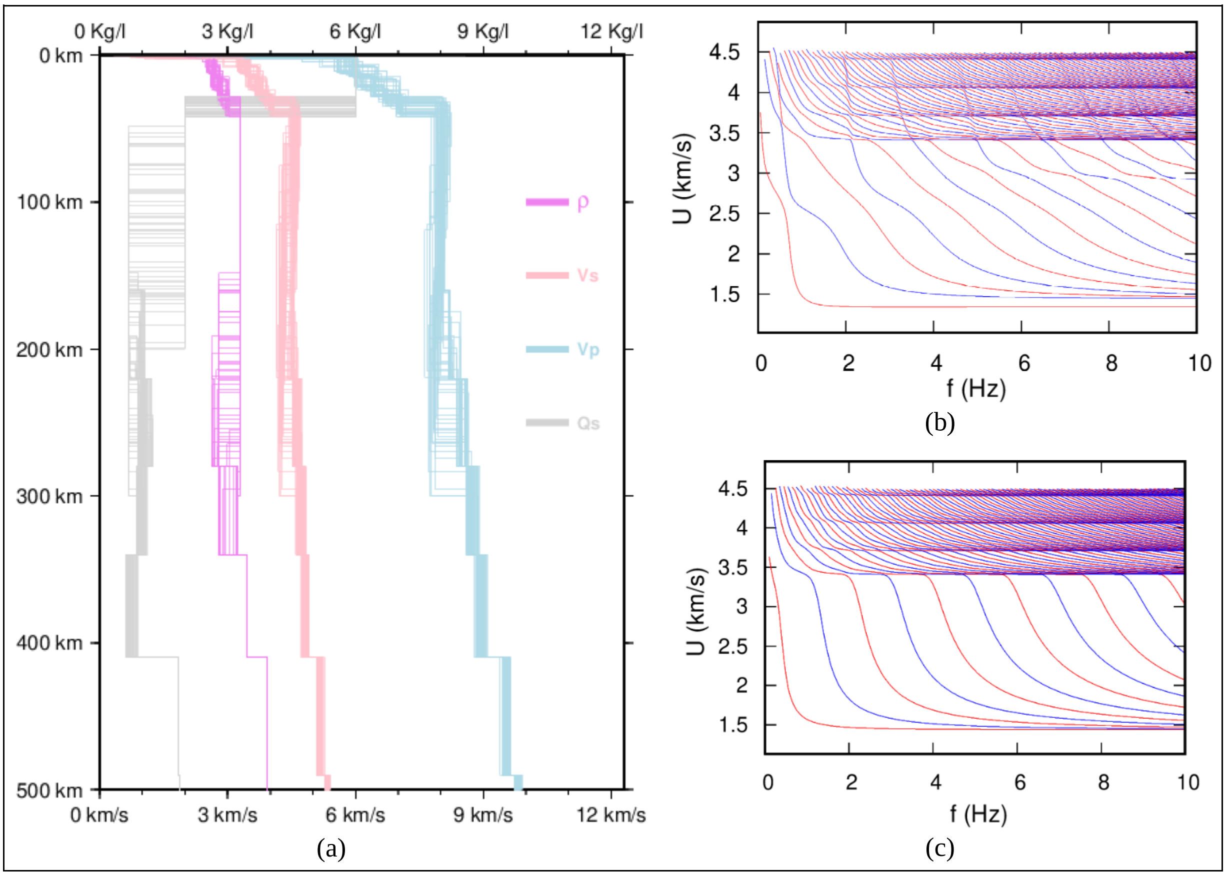

Fig. 8. (a) Overlay structural model is used for this computation (b) Dispersion curve for Rayleigh wave and (c) Dispersion curve for Love wave

2.3. Computation of Synthesis Seismogram

The advantage of NDSHA over PSHA standards is the calculation of strong ground motion parameters based on a simulation of a realistic synthetic seismogram. The simulation results depend on the computational method, source definition, and structural models. NDSHA calculation requires a lot of synthetic seismograms equal to the number of source-receiver paths. Therefore, an efficient computational method is applied without reducing the accuracy of calculations and considering structural model and the source definition parameters such as focal mechanism. The choice of the correct method is the modal summation technique. As the name suggests, the strong ground motion will be obtained from the sum of the modal and the solution for each component and mode is written in equation (1)

$$ {}^{m}U_R(r,z,\omega)=\frac{e^{\frac{-3}{4}i\pi}}{\sqrt{2\pi}}\left[\chi_R(h_s,\varphi)S(\omega)\frac{\sqrt{k_R}e^{-ik_R r-\omega r C_{2R}}}{\sqrt{r}}\frac{\epsilon_0 u_x(z,\omega)}{2c_R v_{gR} I_{1R}}\right]_m \quad {}^{m}U_L(r,z,\omega) = \frac{e^{\frac{-3}{4}i\pi}}{\sqrt{2\pi}}\left[\chi_L(h_s,\varphi)S(\omega)\frac{\sqrt{k_L}e^{-ik_L r-\omega r C_{2L}}}{\sqrt{r}}\frac{u_x(z,\omega)}{2c_L v_{gL} I_{1L}}\right]_m \quad {}^{m}U_Z(r,z,\omega)={}^{m}U_R(r,z,\omega)\frac{e^{\frac{-i\pi}{2}}}{\epsilon_0} \qquad (1) $$

Where R, L, and Z are related to the radial, transverse, and vertical wave components. The radial and vertical components are contributions from the Rayleigh wave and transversal component from the Love wave. The factor of c_R is the phase velocity, V_g group velocity, C_2 phase attenuation, hs focal depth, S(ω) is the spectral source function, and χ_R (h_s, φ) is the radiation pattern. Details explanation can be seen in (Panza et al., 2001, Panza et al., 2020, Hu and Zhu, 2024, Vaccari and Magrin 2022).

3.Results and Discussion

3.1. Synthesis Seismogram and Waveform Observation

Real observation waveform data in the field is complicated process from the complex rupture process that propagates in the complex structural model until it is received in the field by the instrumental accelerometer receiver. The digital waveform data that we obtain in the field is also influenced by instrument response. It cannot be the same as a synthetic seismogram using several assumptions. The local site effect will be disturbed significantly if the instrumental station receiver deploy on a thick sedimentary layer (Panza et al., 2021). However, synthetic seismogram must be verified by real observation in the field. The digital recorded of acceleration waveform was obtained courtesy of BMKG (Irwandi et al., 2018b) as shown in Fig. 9.

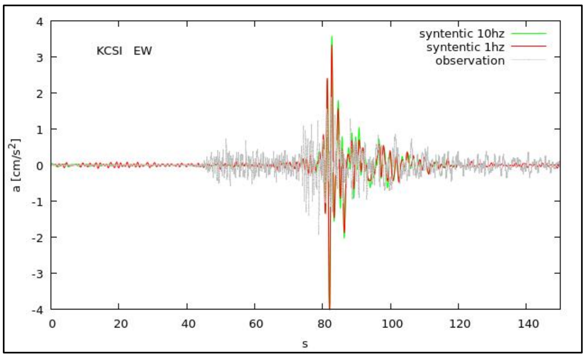

Fig. 9. The recorded accelerogram for KCSI (Kotacane BMKG station)

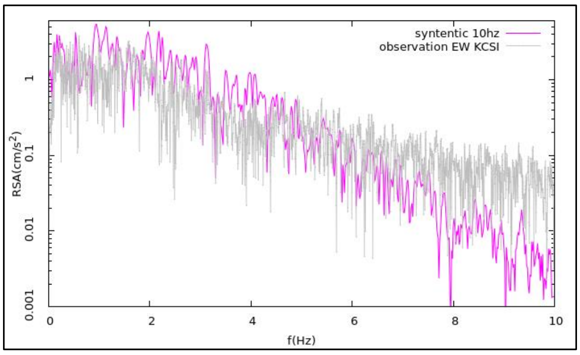

Fig. 10. The related response sprectral acceleration (RSA).

The waveform (Fig. 9) being compared is for the Pidie Jaya earthquake source, the last earthquake from table 1, on 7 December 2016 M6.5, located 5,28 ° N, 96.17 ° E with a focal depth 13.5 km as classification shallow earthquake. The receiver Kotacane station (KCSI) is selected because the collocated station has seismometers and accelerometers at the same location at 3.52°N 97.77°E with epicentral distance 263 km. Besides, the site is located on a thin sediment layer that was relatively less local site effect than other available stations located on tick sedimentary layers.

From waveform in time domain as shown in Fig. 9, we can also produce the spectrums in the frequency domain from the time series data in such domains (Irwandi et al., 2018c). In the summation mode technique, synthetic seismograms generated from the source definition also depend on the structural models. So the spectrum depends on the response of the 1D structural model, thus named response spectra. Fig. 10 shows the Fast Fourier Transform (FFT) response spectra result from the waveform data. RSA values are useful for practical engineering purposes.

The results of synthetic seismogram calculations and field measurement results from the 2016 Pidie Jaya earthquake show that the compuation results already have adequate accuracy, Fig. 9. RSA seems at each component with relatively good suitability for low frequency but underestimated for high frequency using a logarithmic scale. While RSV has suitability in high and low frequencies when compared to RSA as shown in Fig. 10.

We successfully verified the synthetic seismograms from the modal summation technique with instrumental waveforms. Based on the technique for generating synthetic seismograms, the regional scale NDSHA calculation process is carried out using many source definition distributions as obtained in Fig. 5. There will be very many source-receiver paths that must be calculated as the number of synthetic seismograms as the number of sources multiply by the number of receivers. If efficiency is not carried out, this is will computational costly to calculate all synthetic seismograms. The efficiency has been carried out by limiting the path distance, which is a function of the source magnitude.

3.2. NDSHA Geospatial map

The primary computation part in calculating the dispersion curve and synthetic seismogram still uses the original version because the mathematical computation algorithm is still difficult to understand. The updated program is successfully integrated with the original program because we carefully follow the input format for synthetic seismogram computation. NDSHA maps can be obtained from extraction of the synthetic seismogram by providing all the inputs in the form of source definition, structural model, and parameter files as shown in Fig. 11. We can also know the location of the source and focal mechanism that contributes to the PGA as shown in Fig. 12.

The results of NDSHA calculations in Fig. 11 show that PGA should address sensitive to structural crust models, this was not found in the PSHA procedure. Nowadays, the results of tomography can improve the model of crust structure accuracy. So when using the standard methods of PSHA to calculate seismic hazard maps, we will lack accuracy compared to using a NDSHA method that can involve structural models information in Indonesia.

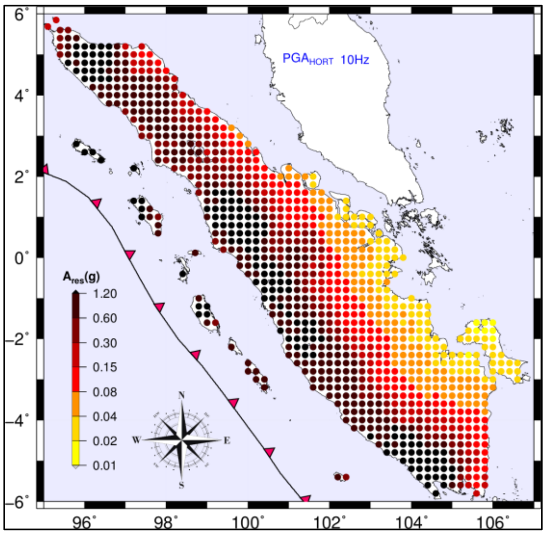

Fig. 11. Horizontal Peak Ground Acceleration from NDSHA computation.

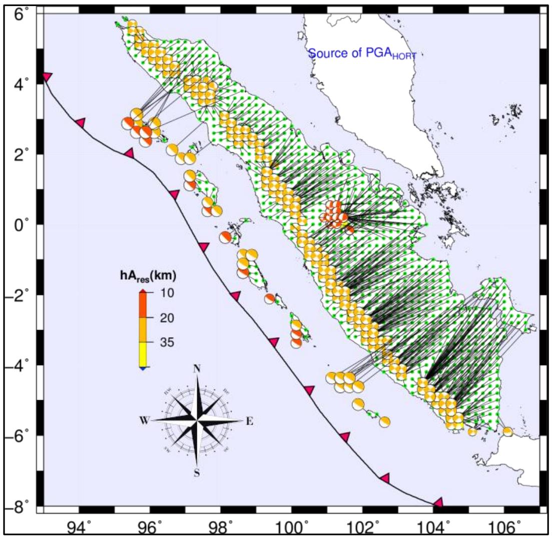

Fig. 12. The most significant contribution for PGA for each location or receiver station.

Fig. 11 shows that the maximum acceleration for the residual horizontal component of PGA has a maximum value scale of 1.2 g. It can be seen that high PGA occurs on the side close to the subduction, and all islands in the forearc basin have relatively high PGA values. In addition, relatively high acceleration values are found on the Great Sumatra Fault line. Meanwhile, those on the east coast of Sumatra have relatively low PGA values, except for the east coast of Aceh province. The low PGA values are consistent with the relatively far position from the Sumatra Fault and Sunda Subduction Zone.

The distance of the maximum earthquake source that contributes to PGA on the east coast of Sumatra with the strike-slip earthquake source of the Sumatra Fault is shown in Fig. 6b. The islands above the forearc basin have significant earthquake sources below the subduction area. The main Sumatra island has significant earthquake sources that can come from the Sumatra Fault or the subduction zone for the area on Sumatra Island. Even significant earthquake sources for the east coast of Sumatra can come from subduction.

In general, the islands above the forearc basin, the west coast of Sumatra, and the central route passed by the Sumatran fault are highly seismically hazard-prone areas, while the area on the east side is a safe zone. Even Bangka Island is one of the low seismic hazard areas with a PGA of less than 0.02g and is very suitable for the location of construction of a nuclear power plant.

3.3. Comparison with PSHA 2017

Although the NDSHA method involves a complex calculation process requiring extensive information on earthquake sources and structural models, as well as computations based on realistic computational seismic wave propagation, the method officially adopted by the Indonesian government remains PSHA (Irwandi et al., 2020), as issued by the Ministry of Public Works and Housing (PUPR). When this paper was written, the official seismic hazard map was PuSGeN 2017.

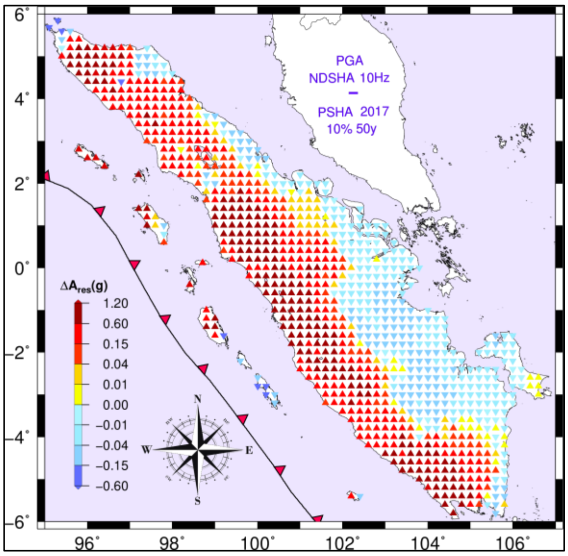

Fig. 13. The difference PGA for NDSHA and PSHA 2017 for 10% exceedance probability over 50

Since it is based on the PSHA method, this map provides several PGA values with 2% and 10% exceedance probabilities over 50 years (Irwandi et al., 2019). In this study, we compare PGA with a 10% exceedance probability over 50 years from PSHA with the results from NDSHA. The difference between PGA values from NDSHA (Figure 11) and PGA values from PSHA, as published by PUPR (2017 edition), is shown in Figure 13.

Figure 13 generally shows that PGA values from NDSHA are higher than those from PSHA in areas near the Sumatran Fault but lower in regions farther from the fault. This suggests that PGA values from NDSHA attenuate more rapidly with distance compared to PGA values from PSHA.

For Banda Aceh, located at the northern tip of Sumatra Island, the PGA values from PSHA are lower than those obtained from NDSHA. Meanwhile, there is significant variation in the forearc islands—some islands show PGA values from NDSHA exceeding those from PSHA, while others show the opposite trend.

4. Conclusion

The verification analysis of modal summation synthetic seismograms computation with observation waveforms of the 2016 Pidie Jaya earthquake recorded at the Kotacane BMKG station is in agreement, with slight differences due to site and sedimentary basin layer effects. Based on the synthetic seismogram computation process, the PGA value of a point can be calculated by calculating all seismic sources that significantly influence an observation point. The precise seismic hazard maps based on realistic physical computation using the NDSHA regional scale has been done to the island of Sumatra. The obtained NSHA map shows a distribution of PGA values that is consistent with the distance of observation to the seismic source. The west coast of Sumatra part has a high seismic hazard prone area with PGA range from 0.6-1.2g. On the other hand, the east coast is a low seismic hazard area with PGAs ranging from 0.01 to 0.04g, except almost the whole Aceh province is a high seismic hazard area.

Comparing the advantages of these two methods is not straightforward due to their fundamentally different approaches: deterministic (NDSHA) vs. probabilistic (PSHA). However, by selecting a specific PGA exceedance probability, such as 2% or 10%, and comparing it with measured ground motion intensity data from the field, further research can be conducted to explore the strengths of each method in greater depth.

Structural models used for the Sumatra NDSHA input on the crust layer are remain using a global model, so Sumatra island's resolution and accuracy can still be improved. Therefore, tomography studies to input more rigorous structural models for the crust layer are being implemented. Based on Indonesia's condition that high seismic risk and the successful application to the NDSHA regional scale of Sumatra, it is strongly recommended to apply similar research and application of NDSHA for entire Indonesia.

Acknowledgements

This paper work is financially supported by "PUU" scheme Universitas Syiah Kuala, Ministry of Education and Culture, Number: 267/UN11/SPK/PNBP/2020 date March 17, 2020.

References

Adhari, M.R. and Hidayat, R., 2023. A geological overview of the limestone members of the Woyla Group of Sumatra, Indonesia. Journal of Geoscience, Engineering, Environment, and Technology, 8(3), pp.189-195. https://doi.org/10.25299/jgeet.2023.8.3.12190

Amir, H., Bijaksana, S., Dahrin, D., Nugraha, A.D., Arisbaya, I., Pratama, A. and Suryanata, P.B., 2021. Subsurface structure of Sumani segment in the Great Sumatran Fault inferred from magnetic and gravity modeling. Tectonophysics, 821, p.229149.

Bahrampouri, M., Rodriguez-Marek, A. and Green, R.A., 2021. Ground motion prediction equations for significant duration using the KiK-net database. Earthquake Spectra, 37(2), pp.903-920.

Bhat, G.R., Balaji, S. and Yousuf, M., 2023. Tectonic geomorphology and seismic hazard of the east boundary thrust in northern segment of the Sunda–Andaman subduction zone. Natural Hazards, 116(1), pp.401-423.

Dalton, C.A., Ekström, G., and Dziewonski, A.M. 2008. The Global Attenuation Structure of The Upper Mantle. Journal of Geophysical Research 113. DOI:10.1029/2007JB005429.

Dwikorianto, T., Daud, Y., Martha, A.A. and Juanda, A.A., 2023. Ambient Noise Data Processing to Obtain Group Velocity for Subsurface Structure Identification: Preliminary Research in Hululais Geothermal Field, Sumatra, Indonesia. Journal of Geoscience, Engineering, Environment, and Technology, 8(02-2), pp.67-71. https://doi.org/10.25299/jgeet.2023.8.02-2.13883

Elgabry, M.N., Hassan, H.M. and Hussein, H., 2022. Recent applications of NDSHA: seismic input for high rise buildings in Egypt's New Administrative Capital. In Earthquakes and Sustainable Infrastructure (pp. 239-253). Elsevier.

Fadhlurrohman, R., Syafriani, S., Raharjo, F.D., Asnawi, Y. and Ahadi, S., 2024. Coulomb Stress Change of Active Fault in South Sumatra Region Revealed from Kerinci Earthquake October 06, 1995 Mw 6.7 and Sungai Penuh Earthquake October 01, 2009 Mw 6.6. Journal of Geoscience, Engineering, Environment, and Technology, 9(3), pp.378-384. https://doi.org/10.25299/jgeet.2024.9.3.19273

Hassan, H. M., Romanelli, F., Panza, G. F., ElGabry, M. N., & Magrin, A. (2017). Update and sensitivity analysis of the neo-deterministic seismic hazard assessment for Egypt. Engineering Geology, 218, 77-89.

Hu S, Zhu L. 2024. Computing theoretical seismograms from a point source in a spherical multilayered medium. Seismological Research Letters. 2024 Jan 1;95(1):448-57.

Hu, H., Zhao, D., Lin, J. and Pilia, S., 2023. A slab window beneath North Sumatra revealed by P- wave mantle tomography. Journal of Geophysical Research: Solid Earth, 128(6), p.e2022JB025976.

Hutchings, S.J. and Mooney, W.D., 2021. The seismicity of Indonesia and tectonic implications. Geochemistry, Geophysics, Geosystems, 22(9), p.e2021GC009812.

Irsyam, M., Cummins, P.R., Asrurifak, M., Faizal, L., Natawidjaja, D.H., Widiyantoro, S., Meilano, I., Triyoso, W., Rudiyanto, A., Hidayati, S. and Ridwan, M., 2020. Development of the 2017 national seismic hazard maps of Indonesia. Earthquake Spectra, 36(1_suppl), pp.112-136.

Irwandi, I., Muzli., Muksin and Jamaluddin, K. (2018a) "GMPE based Shakemap Generation of Peak Ground Motion and Intensity Maps for Pidie Jaya Earthquake," Journal of Physics, vol. 1120, p. 012092.

Irwandi, I., Rusydy, I., Muksin, U., & Rudyanto, A. (2018b). Synthetic accelerogram of modal summation technique and its validation with the Pidie Jaya earthquake data. In AIP Conference Proceedings (Vol. 1987, No. 1, p. 020026). AIP Publishing LLC.

Irwandi, I., Rusydy I., Muksin, U., and Rudyanto, A (2018c). "Response Spectra Analysis of the Modal Summation Technique Verified by Observed Seismometer and Accelerometer Waveform Data of the M6.5 Pidie Jaya Earthquake," in Materials Science and Engineering.

Irwandi, I., Idris, Y., Muksin., Jamaluddin, K., Zulfakriza, Joni., and Muzli. (2019) "Realistic Shakemap M6.5 Pidie Jaya Earthquake 7 Desember 2016 Based on Modal Summation Technique," in Earth and Environmental Science, 2019.

Irwandi, I., Umar, M., Khaizal, J., Asrurifak, M., Usama, F., & Ridwan, M. (2020). The Neo-Deterministic Seismic Hazard map (NDSHA) of Sumatra compared with official 2010 and 2017 derived from PSHA method. In IOP Conference Series: Materials Science and Engineering (Vol. 712, No. 1, p. 012017). IOP Publishing.

Irwandi, I., Muksin, U., & Simanjuntak, A. V. (2021). Probabilistic seismic hazard map analysis for Aceh Tenggara district and microzonation for Kutacane city. In IOP Conference Series: Earth and Environmental Science (Vol. 630, No. 1, p. 012001). IOP Publishing.

Irwandi, I., 2022. Application of neodeterministic seismic hazard analysis to Sumatra. In Earthquakes and Sustainable Infrastructure (pp. 601-615). Elsevier.

Jacob, J., Dyment, J., Ghosal, D. and Dewangan, P., 2021. Strike-slip seismicity at the Andaman-Sumatra Subduction Zone: Role of the fracture zones and age of the subducting lithosphere. Tectonophysics, 811, p.228862.

Liu, Y., Suardi, I., Huang, X., Liu, S. and Tong, P., 2021. Seismic velocity and anisotropy tomography of southern Sumatra. Physics of the Earth and Planetary Interiors, 316, p.106722.

Magrin, A., Parvez, I.A., Vaccari, F., Peresan, A., Rastogi, B.K., Cozzini, S., Bisignano D., Romanelli, F., Choudhury, P., Roy., K.S., Mir, R.R., and Panza, G.F. (2016). Neo-deterministic Definition of Seismic and Tsunami Hazard Scenarios for the Territory of Gujarat (India). In Earthquakes and Their Impact on Society (pp. 193-212). Springer International Publishing.

Marzocchi, W. and Meletti, C., 2024. PSHA: Does it deal with what it is or what we want it to be?. Seismological Research Letters, 95(3), pp.1469-1472.

McKenna, P. (2011). Earthquake engineer: Earthquakes don't kill, but buildings do. New Scientist, 210(2813), 23.

Muksin, U., Arifullah, A., Simanjuntak, A.V., Asra, N., Muzli, M., Wei, S., Gunawan, E. and Okubo, M., 2023. Secondary fault system in Northern Sumatra, evidenced by recent seismicity and geomorphic structure. Journal of Asian Earth Sciences, 245, p.105557.

Natul, Al Shida, and Heliani, L.S., 2022. A comparison of geologic structure detection of Sumatera Island using goce satellite gravity data and Sgg-Ugm-2 data. Journal of Geoscience, Engineering, Environment, and Technology, 7(3), pp.95-101. https://doi.org/10.25299/jgeet.2022.7.3.8863

Osagie, A.U. and Ahmad Abir, I., 2021. Seismic tomographic imaging of P wave velocity perturbation beneath Sumatra, Java, Malacca Strait, Peninsular Malaysia and Singapore. Journal of Earth System Science, 130(1), p.23.

Panza, G.F., Irikura, K., Kouteva, M., Peresan, A., & Wang, Z. 2012. Advanced seismic hazard assessment. Pure and Applied Geophysics, 169, 1-28. https://doi.org/10.1007/s00024-011-0360-5.

Panza, G.F. and Bela, J., 2020. NDSHA: A new paradigm for reliable seismic hazard assessment. Engineering Geology, 275, p.105403.

Panza, G., Kossobokov, V.G., Laor, E. and DeVivo, B. eds., 2021. Earthquakes and sustainable infrastructure: neodeterministic (NDSHA) approach guarantees prevention rather than cure. Elsevier.

Panza, G.F., Romanelli, F., & Vaccari, F. 2001. Seismic wave propagation in laterally heterogeneous anelastic media:

Theory and applications to seismic zonation. In R.D. James (Ed.), Advances in geophysics (Vol. 43, pp. 1-95). Academic Press. https://doi.org/10.1016/S0065-2687(02)80003-9.

Parvez, I. A., Magrin, A., Vaccari, F., Mir, R. R., Peresan, A., & Panza, G. F. (2017). Neo-deterministic seismic hazard scenarios for India—a preventive tool for disaster mitigation. Journal of Seismology, 21(6), 1559-1575.

Pasyanos, M.E., Masters, T.G., Laske, G., and Ma, Z. (2014). LITHO1.0: An Updated Crust and Lithospheric Model of the Earth. J. Geophys. Res., 119 (3), 2153-2173. DOI: 10.1002/2013JB010626.

Pendiaman, N., Opon, J. and Cantila, K., 2024. Development of new seismic hazard maps of the Philippines using the neo-deterministic seismic hazard assessment approach. Rendiconti Lincei. Scienze Fisiche e Naturali, 35(2), pp.523-537.

Pesicek, J.D., Thurber, C.H., Widiyantoro, S., Zhang, H., DeShon, H.R., and Engdahl, E.R. (2010). Sharpening the Tomographic Image of the Subducting Slab Below Sumatra, the Andaman Islands and Burma. Geophys. J. Int. (2010) 182, 433–453.

PuSGeN, National Earthquake Study Center Team, 2017. Peta Sumber dan Bahaya Gempa Indonesia Ministry of Public Works and Public Housing

Putra, A.S., Nugraha, A.D., Sahara, D.P., Zulfakriza, Z., Puspito, A.N.T., Muttaqy, F., Supendi, P. and Daryono, D., 2023. Seismicity pattern of the great sumatran fault system from hypocenter relocation of regional seismic network. Indonesian Journal on Geoscience, 10(1), pp.83-95.

Rafie, M.T., Sahara, D.P., Cummins, P.R., Triyoso, W. and Widiyantoro, S., 2023. Stress accumulation and earthquake activity on the Great Sumatran Fault, Indonesia. Natural Hazards, 116(3), pp.3401-3425.

Shamim, S., Khan, P.K., Mohanty, S.P. and Mohanty, M., 2021. Andaman–Nicobar–Sumatra margin revisited: analysis of the lithospheric structure and deformation based on gravity modeling and distribution of seismicity. Surveys in Geophysics, 42, pp.239-275.

Storchak, D.A., Harris, J., Brown, L., Lieser, K., Shumba, B., Di Giacomo, D. (2020) Rebuild of the Bulletin of the International Seismological Centre (ISC)—part 2: 1980–2010. Geosci. Lett. 7: 18, https://doi.org/10.1186/s40562-020-00164-6. http://www.isc.ac.uk

Vaccari, F. and Magrin, A., 2022. A user-friendly approach to NDSHA computations. In Earthquakes and Sustainable Infrastructure (pp. 215-237). Elsevier.

Wei, J., Liu, Q., Chen, L., Wei, S. and Zhao, L., 2024. A novel 3- D seismic scattering and intrinsic attenuation tomography and its application to Northern Sumatra. Journal of Geophysical Research: Solid Earth, 129(11), p.e2024JB029116.

Widiyantoro, S., Supendi, P., Rawlinson, N., Daryono, M.R. and Rosalia, S., 2024. A note on the seismicity of Sumatra, western Sunda Arc, Indonesia, in relation to the potential for back-arc thrusting. Scientific Reports, 14(1), p.13115.

Yadav, R. and Tiwari, V.M., 2020. Lithospheric Framework of Sumatra–Andaman Subduction Zone—A Review. The Andaman Islands and Adjoining Offshore: Geology, Tectonics and Palaeoclimate, pp.137-159.

Zanetti, L., Chiffi, D. and Petrini, L., 2023. Philosophical aspects of probabilistic seismic hazard analysis (PSHA): a critical review. Natural Hazards, 117(2), pp.1193-1212.

Zhang, Y., Wu, Z., Romanelli, F., Vaccari, F., Jiang, C., Gao, S., Li, J., Kossobokov, V.G. and Panza, G.F., 2021. Next-generation EEW empowered by NDSHA: From concept to implementation. Geosciences, 11(11), p.473.

Zhang, Y., Wu, Z., Romanelli, F., Vaccari, F., Peresan, A., Li, J. and Panza, G.F., 2023. Earthquake Early Warning System (EEWS) empowered by Time- Dependent Neo- Deterministic Seismic Hazard Assessment (TD- NDSHA). Terra Nova, 35(3), pp.230-239.

© 2025 Journal of Geoscience, Engineering, Environment and Technology. All rights reserved. This is an open access article distributed under the terms of the CC BY-SA License (http://creativecommons.org/licenses/by-sa/4.0/).